2006

# Synthesis of High-Temperature Stable Anatase TiO2 Photocatalyst

Suresh Pillai
*Technological University Dublin*, suresh.pillai@tudublin.ie

Declan McCormack
*Technological University Dublin*, Declan.mccormack@tudublin.ie

Michael Seery
*Technological University Dublin*, michael.seery@tudublin.ie

Pradeepan Periyat
pradeepan.periyat@tudublin.ie

Steven Hinder

# Synthesis of High-Temperature Stable Anatase $TiO_2$ Photocatalyst

**Suresh C. Pillai,*,† Pradeepan Periyat,†,‡ Reenamole George,†,‡ Declan E. McCormack,‡ Michael K. Seery,‡ Hugh Hayden,† John Colreavy,† David Corr,§ and Steven J. Hinder⊥**

*Centre for Research in Engineering Surface Technology (CREST), FOCAS Institute, Dublin Institute of Technology, Camden Row, Dublin 8, Ireland, School of Chemical and Pharmaceutical Sciences, Dublin Institute of Technology, Kevin Street, Dublin 8, Ireland, NTera Ltd., 58 Spruce Avenue, Stillorgan Industrial Park, Blackrock, Co., Dublin, Ireland, and The Surface Analysis Laboratory, School of Engineering, University of Surrey, Guildford, Surrey, GU2 7XH, United Kingdom*

*Received: September 12, 2006; In Final Form: November 9, 2006*

In the absence of a dopant or precursor modification, anatase to rutile transformation in synthetic $TiO_2$ usually occurs at a temperature of 600−700 °C. Conventionally, metal oxide dopants (e.g., $Al_2O_3$ and $SiO_2$) are used to tune the anatase to rutile transformation. A simple methodology is reported here to extend the anatase rutile transformation by employing various concentrations of urea. XRD and Raman spectroscopy were used to characterize various phases formed during thermal treatment. A significantly higher anatase phase (97%) has been obtained at 800 °C with use of a 1:1 $Ti(OPr)_4$:urea composition and 11% anatase composition is retained even after calcining the powder at 900 °C. On comparison a sample that has been prepared without urea showed that rutile phases started to form at a temperature as low as 600 °C. The effect of smaller amounts of urea such as 1:0.25 and 1:0.5 $Ti(OPr)_4$:urea has also been studied and compared. The investigation concluded that the stoichiometric modification by urea 1:1 $Ti(OPr)_4$:urea composition is most effective in extending the anatase to rutile phase transformation by 200 °C compared to the unmodified sample. In addition, BET analysis carried out on samples calcined at 500 °C showed that the addition of urea up to 1:1 $Ti(OPr)_4$:urea increased the total pore volume (from 0.108 to 0.224 $cm^3/g$) and average pore diameter (11 to 30 nm) compared to the standard sample. Samples prepared with 1:1 $Ti(OPr)_4$:urea composition calcined at 900 °C show significantly higher photocatalytic activity compared to the standard sample prepared under similar conditions. Kinetic analysis shows a marked increase in the photocatalytic degradation of rhodamine 6G on going from the standard sample (0.27 $min^{-1}$, decoloration in 120 min) to the urea-modified sample (0.73 $min^{-1}$, decoloration in 50 min).

## 1. Introduction

Nanocrystalline titania ($TiO_2$) has received significant attention in the last few decades due to the photoinduced electron-transfer properties associated with the anatase metastable phase.[1−3] Titania usually exists in three different forms: anatase (tetragonal, $a = b = 3.78$ Å; $c = 9.50$ Å), rutile (tetragonal, $a = b = 4.58$ Å; $c = 2.95$ Å), and brookite (rhombohedral, $a = 5.43$ Å; $b = 9.16$ Å; $c = 5.13$ Å). These crystalline structures consist of $[TiO_6]^{2-}$ octahedra, which share edges and corners in different manners while keeping the overall stoichiometry as $TiO_2$.[4−7] Even though anatase has more edge sharing octahedra, the interstitial spaces between octahedra are larger, which makes rutile denser than anatase (the density of anatase is 3.84 $g/cm^3$ and that of rutile is 4.26 $g/cm^3$).[4−7] Among the various phases of titania reported, anatase shows a better photocatalytic activity and antibacterial performance.[8−12] A stable anatase phase up to the sintering temperature of the ceramic substrates is most desirable for applications on anti-bacterial self-cleaning building materials (e.g., bathroom tile, sanitary ware, etc.).[13−15] These applications require high-purity titania with a definite phase composition.[13−15] The production of high-photoactivity material with high-temperature anatase phase stability is one of the key challenges in smart coating technology. Anatase-to-rutile transformation in pure titania usually occurs at 600 to 700 °C.[16−18] Phase transition to rutile is nonreversible due to the greater thermodynamic stability of rutile phase.[19−20] Researchers at Toto Ltd. recently reported[21] a method to produce photoactive titania-Ag coatings on ceramic materials. The composition contains up to 7% anatase present at 900 °C.[21] Any improvement in the anatase phase composition at these high temperatures is expected to show a higher photocatalytic activity.[21] Conventionally metal oxide doping is used to extend the anatase-to-rutile transformation temperature above 700 °C.[22−26] Various metal oxide dopants such as $Al_2O_3$, NiO, $SiO_2$, $ZrO_2$, ZnO, and $Sb_2O_5$ have already been studied to assess the effect on both anatase-to-rutile transformation and alteration of modification on textural properties of titania.[22−26] Formation of secondary impurity phases (e.g., $Al_2TiO_5$, $NiTiO_3$) at high temperature is the main disadvantages of this technique. Modifying the precursor characteristics by employing chelating agents is another approach attempted earlier to obtain titania having specific properties.[27−28] Recent research showed that urea has little effect on the phase formation in titania.[29] Previously, urea has been employed to improve the pore parameters and morphology by utilizing it as a pore-forming agent.[29−31] Zheng et al. reported preparation of mesoporous titania via sol-gel

* Address correspondence to this author. E-mail: suresh.pillai@dit.ie.
† FOCAS Institute, Dublin Institute of Technology.
‡ School of Chemical and Pharmaceutical Sciences, Dublin Institute of Technology.
§ NTera Ltd.
⊥ School of Engineering, University of Surrey.

10.1021/jp065933h CCC: $33.50 
Published on Web 00/00/0000 PAGE EST: 6.1

reactions by using urea as a template.[32] Bakardjieva et al. showed the formation of $TiO_2$ nanocrystals from titanyloxy chloride by using urea as a precipitating agent.[33] Also there are recent reports published which explain the visible light activity of titania by doping with nitrogen where urea or thiourea is used as a precursor.[34−37] However, there is no systematic study available in the literature on the effect of various concentrations of urea on high-temperature stability of anatase. Here in our study the titania precursor gel has been prepared by hydrolysis and condensation reaction of titanium isopropoxide ($Ti(OPr)_4$) with various mole ratios of urea. The phase transformation during heat treatment was investigated by X-ray powder diffraction (XRD). The current study showed that a major anatase phase (up to 97%) can be retained at 800 °C by modifying titanium isopropoxide with urea. On the other hand, the standard titania showed the presence of rutile at a temperature as low as 600 °C. This method has therefore been found to be effective in extending the anatase-to-rutile phase transformation by at least 200 °C without using any metal oxide additives. Titania composition prepared by 1:1 $Ti(OPr)_4$:urea molar ratio calcined at 900 °C shows significantly higher photocatalytic activity compared to the standard sample. Degradation kinetics on a model dye, rhodamine 6G, demonstrate that the urea-modified sample is more than three times as efficient as the standard sample, a fact attributed to the increased amount of anatase in the urea-modified sample.

## 2. Experimental Methods

The reagents used in this study were titanium isopropoxide (Aldrich) and urea (Aldrich). In a typical experiment to synthesize 1:1 titania precursor:urea solution, 46.80 mL of titanium isopropoxide ($Ti(OPr)_4$) was added into 412 mL of isopropanol. To the above solution, 10 g of urea dissolved in 70 mL of water was added. The solution was then stirred for 5 min and aged for 2 h at room temperaturre. It was then dried at 80 °C for 24 h. The dried powder was calcined at a constant heating rate of 5 deg/min at 500, 600, 700, 800, 900, and 1000 °C and held at these temperatures for 2 h.

The same procedure is adopted to synthesize 1:0.25 and 1:0.5 $Ti(OPr)_4$:urea samples. A standard sample without urea was also prepared to compare the results. XRD patterns of the calcined gels were obtained with a Siemens D 500 X-ray diffractometer in the diffraction angle range $2\theta = 20-70°$, using Cu K$\alpha$ radiation. The amount of anatase in the sample was estimated by using the Spurr equation (eq 1)[38]

$$F_A = 100 - \left(\frac{1}{1 + 0.8(I_A(101)/I_R(110))}\right)100 \qquad (1)$$

where $F_A$ is the mass fraction of anatase in the sample and $I_A$(101) and $I_R$(110) are the integrated main peak intensities of anatase and rutile, respectively.

The BET (Brunauer, Emmett, and Teller) surface area measurements and pore analysis were carried out by nitrogen adsorption with use of a Micromeritics Gemini 2375 surface area analyzer. The measurements were carried out at liquid nitrogen temperature after degassing the powder samples for 1 h 30 min at 200 °C.

Differential Scanning Calorimetry (DSC) measurements were carried out with a Rheometric Scientific DSC QC. A small amount of the dried sample (less than 3 mg) was heated from room temperature (25 °C) to 400 °C at a constant heating rate of 10 deg/min.

The FTIR spectra of the gel dried at 80 °C was measured by using a Spectrum GX-FTIR spectrophotometer in the wave number range 4000−400 $cm^{-1}$, using 70 scans per sample.

X-ray Photoelectron Spectroscopy (XPS) analyses were performed on a Thermo VG Scientific (East Grinstead, UK) Sigma Probe spectrometer. The instrument employs a monochromated Al K$\alpha$ X-ray source ($h\nu = 1486.6$ eV), which was used at 140 W. The area of analysis was approximately 500 $\mu$m diameter for the samples analyzed. For survey spectra a pass energy of 100 eV and a 0.4 eV step size were employed. For $C_{1s}$ and $Ti_{2p}$ high-resolution spectra a pass energy of 20 eV and a 0.1 eV step size were used. For $O_{1s}$ high-resolution spectra a pass energy of 20 eV and a 0.2 eV step size were used. For $N_{1s}$ high-resolution spectra a pass energy of 50 eV and a step size of 0.2 eV were used. Charge compensation was achieved by using a low-energy electron flood gun. Quantitative surface chemical analyses were calculated from the high-resolution core level spectra, following the removal of a nonlinear Shirley background. The manufacturer's Avantage software was used, which incorporates the appropriate sensitivity factors and corrects for the electron energy analyzer transmission function.

**Photocatalysis Studies.** In a typical experiment, a 0.06 g standard sample calcined at 900 °C was dispersed in 50 mL of Rhodamine 6G solutions having a concentration of $5 \times 10^{-6}$ M. The above suspension was irradiated in a Q-Sun Xenon solar simulator chamber (0.68 W/$m^2$ at 340 nm) with stirring. Degradation was monitored by taking aliquots at increasing time intervals. These aliquots were centrifuged and absorption spectra of the samples were recorded. Similar experiments were carried out for urea modified sample calcined at 900 °C. The rate of degradation was assumed to obey pseudo-first-order kinetics and hence the rate constant for degradation, $k$, was obtained from the first-order plot according to eq 2

$$\ln\left(\frac{A_0}{A}\right) = kt \qquad (2)$$

where $A_0$ is the initial absorbance, $A$ is the absorbance after a time ($t$) of the rhodamine dye degradation, and $k$ is the first-order rate constant.

## 3. Results

**3.1. FTIR Spectroscopy.** FTIR spectra of the precursor samples dried at 80 °C have been recorded. The absorption band at 3500−3000 and 1600 $cm^{-1}$ in all spectra indicate hydroxyl group stretching vibrations.[29] The broad peak at 500 $cm^{-1}$ found in the standard and urea modified samples indicates the Ti−O−Ti stretching vibrations.[29] The peak observed at 1035 $cm^{-1}$ corresponds to the Ti−O−C bond. The Ti−O−C bond is predicted to be the result of the interaction between the Ti−O network and the C═O in the urea.[29] The peaks corresponding to Ti−O−C bond increase in intensity when the urea concentration increases (Supporting Information Figure 1). This is a good indication that there is a great degree of interaction between the inorganic and organic components by the condensation reaction. The peak obtained at 1154 $cm^{-1}$ is assigned to the stretching vibration of C−N.[29] The peak obtained at 1453 $cm^{-1}$ is due to the deformation mode of ammonium ions formed by the decomposition of excess urea.[40] FTIR results thus show a strong chelation of urea molecules to the titania precursor. It has been observed that the peaks at 1035 (which is assigned for the Ti−O−C bond) and 1154 $cm^{-1}$ (C−N) were absent above a calcination temperature of 200 °C and all additional peaks except Ti−O stretching are absent above 300 °C.

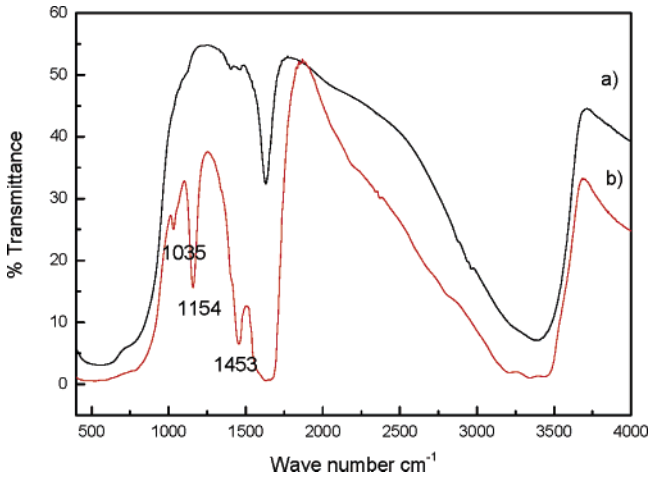


**Figure 1.** FTIR spectra of the 80 °C dried titania precursor: (a) standard sample and (b) sample of 1:1 $Ti(OPr)_4$:urea composition.

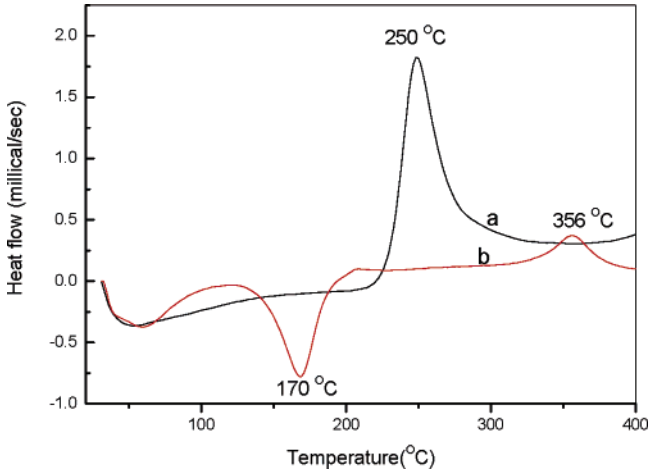


**Figure 2.** Differential scanning calorimetry of (a) standard and (b) sample of 1:1 $Ti(OPr)_4$:urea composition.

**TABLE 1: BET Surface Area Analysis at 500 °C**

| material | surface area ($m^2$/g) | total pore vol ($cm^3$/g) | av pore diameter (nm) ±10% |
|---|---|---|---|
| standard $TiO_2$ sample | 38 | 0.108 | 11 |
| 1:1 $Ti(OPr)_4$:urea composition | 30 | 0.224 | 30 |

**3.2. Differential Scanning Calorimetry (DSC).** Differential Scanning Calorimetry (DSC) studies have been carried out (Figure 2) to investigate the amorphous-to-crystalline transition of the titania precursor. An endothermic peak at 170 °C has been observed for the 1:1 $Ti(OPr)_4$:urea sample and this peak has been assigned as the thermal decomposition of the titania−urea precursor. The exothermic peaks (Figure 2a,b) at 250 and 356 °C respectively for the standard and 1:1 $Ti(OPr)_4$:urea samples indicate the amorphous-to-crystalline formation.[27] It is therefore evident from Figure 2 that the amorphous-to-crystalline formation is delayed in the case of the urea-modified sample. XRD analysis has been conducted to confirm the crystallization characteristics at 250 °C. An amorphous phase was obtained for the 1:1 $Ti(OPr)_4$:urea samples while a crystalline anatase phase was observed for the standard sample (Supporting Information Figure 2).

**3.3. Surface Area Measurements.** BET surface area and total pore volume are calculated at $p/p_0 = 0.99$ by the BET method

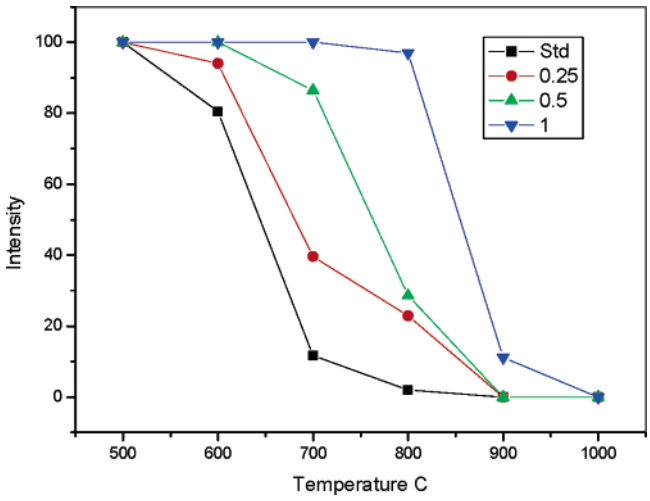


**Figure 3.** Anatase content in the samples calcined at various temperatures.

for the samples calcined at 500 °C. The results are shown in Table 1. Both isotherms for the standard and urea added samples are type IV-like in their behavior (Supporting Information Figure 3). An earlier report[32] shows that the urea is a good pore forming agent so that it will help in the generation of mesoporosity in the titania framework. The current study also confirms that the addition of urea (1:1) increases the pore diameter to 30 nm compared to the 11 nm pore diameter of the standard sample (Table 1). BET analysis of the samples calcined at higher temperatures showed that the 1:1 $Ti(OPr)_4$:urea sample possesses a higher surface area (15 $m^2$/g) at 800 °C compared to the standard sample calcined (5 $m^2$/g) at the same temperature. The surface area of both the 1:1 $Ti(OPr)_4$:urea sample and the standard sample at 900 °C showed surface areas of 5 and 4 $m^2$/g, respectively.

**3.4. XRD Analysis.** Titania precursor samples prepared with urea indicated a significant rise in transformation temperature of anatase to rutile. As the amount of urea increased, the transformation temperature is also raised to higher temperatures (Figure 3).

The weight fraction of the anatase found in the sample was calculated by comparing the XRD integrated intensities of (101) reflection of anatase and (110) reflection of rutile. All the samples heated to 500 °C show only anatase phase (Figure 3). The standard sample showed the formation of rutile at a temperature as low as 600 °C (the anatase content was calculated as 80%). However, all the urea-modified samples except the 1:0.25 (only 6% rutile; 94% anatase) calcined at 600 °C show a complete anatase phase, indicating that a lower percentage of urea has little effect on the anatase rutile transformation (Supporting Information Figure 4).

At 700 °C the standard sample showed rutile as the major phase with 12% anatase (Figure 3) while the samples with 1:0.25 and 1:0.5 $Ti(OPr)_4$:urea composition showed the presence of 40% and 86% anatase, respectively (Supporting Information Figure 5). At 800 °C standard (Figures 3 and 4, and Supporting Information Figure 6), 1:0.25 and 1:0.5 $Ti(OPr)_4$:urea composition showed a lower anatase content (0%, 23%, and 27%, respectively). A significantly high anatase content (97%) was obtained for sample with the highest urea content, i.e., 1:1 $Ti(OPr)_4$:urea, up to a temperature of 800 °C (Figures 3 and 4). All the samples except a sample with the composition of 1:1 $Ti(OPr)_4$:urea turned to fully rutile at 900 °C. The sample with

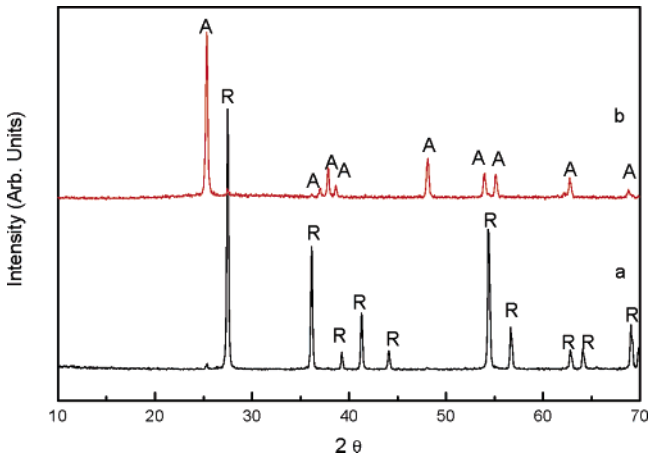


**Figure 4.** XRD of the samples calcined at 800 °C (A = anatase; R = rutile) of (a) standard sample and (b) sample prepared by 1:1 $Ti(OPr)_4$:urea composition.

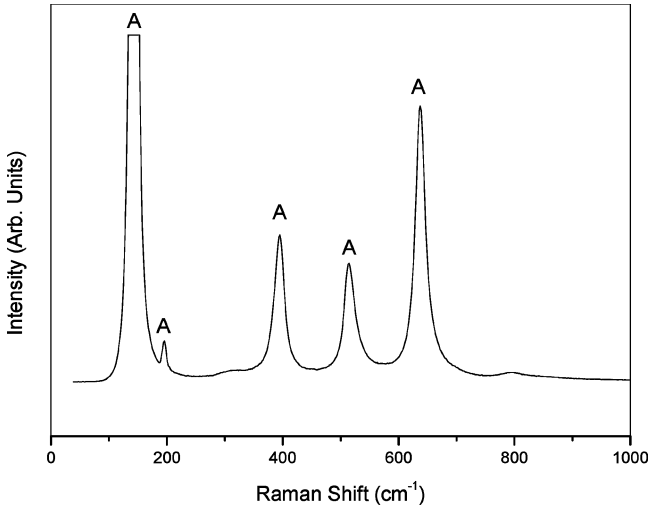


**Figure 5.** Raman spectra of titania sample with 1:1 $Ti(Opr)_4$:urea calcined at 800 °C (A = anatase).

a composition of 1:1 $Ti(OPr)_4$:urea showed 11% anatase at 900 °C (Supporting Information Figure 7).

XRD studies concluded that the modification by urea 1:1 Ti $(OPr)_4$:urea has been effective in increasing the anatase-to-rutile transformation to high temperature.

**3.5. Raman Studies.** Raman spectroscopy was applied as an additional tool to probe the phase formation of standard (Supporting Information Figures 8 and 9) and 1:1 $Ti(OPr)_4$: urea titania samples. Figures 5 and 6 show Raman spectra obtained with samples of composition 1:1 $Ti(OPr)_4$:urea calcined at 800 and 900 °C. According to factor group analysis the anatase phase consists of six and the rutile phase consists of five Raman active modes (i.e., anatase—144, 197, 399, 513, and 639 $cm^{-1}$; rutile—144, 446, 612, and 827 $cm^{-1}$). Figure 5 shows a strong peak at 197 $cm^{-1}$, which is the characteristic peak of the anatase phase. The peak at 197 $cm^{-1}$ appears along with other characteristic rutile phases in Figure 6 indicating the presence of the anatase phase in the 900 °C calcined sample. These two Raman spectra are consistent with the XRD results.

**3.6. X-ray Photoelectron Spectroscopy (XPS).** XPS measurements have been carried out to determine N or C incorporation above 500 °C (Figure 7; Supporting Information Figure 10). The presence of C (ca. 11%) and N (ca. 0.5%) was confirmed in the XPS analysis (Table 2). It was previously reported that the $N_{1s}$ peak will show a binding energy value of

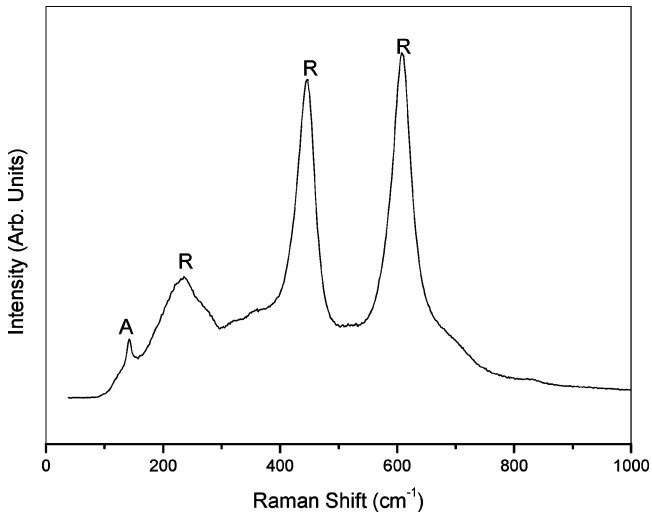


**Figure 6.** Raman spectra of titania sample with 1:1 ($Ti(Opr)_4$:urea) calcined at 900 °C (A = anatase; R = rutile).

400−402 eV and $C_{1s}$ will show a binding energy of 281−287 eV.[41] The signal (Figure 7a) observed at 400 eV was explained previously as a result of the molecular chemisorbed nitrogen.[42,43] However, there was no indication of Ti−N bond formation (396 eV).[42]

Three forms of carbon have been identified previously which are surface adsorbed (287.5 eV), solid solution (285 eV), and the carbide Ti−C (281.5 eV).[41] It can be seen from the XPS spectra (Figure 7b) of $C_{1s}$ that the majority of the carbon present in the $TiO_2$ matrix exists as a solid solution (285 eV). A small surface adsorbed carbon peak is found in all the samples even though the intensity of this peak decreases at 800 °C. There is no indication of the formation of any Ti−C phase. Carbon can locate as a solid solution within the tetrahedral and octahedral interstices existing within the anatase crystal.[41]

**3.7. Photocatalytic Studies.** Photocatalytic studies have been carried out by studying the decomposition reaction of rhodamine dye in the presence of standard and the urea modified samples. The urea modified sample 1:1 $Ti(OPr)_4$:urea shows more than three times the activity of the unmodified titania. The full decolorization of the rhodamine dye occurred within 50 min in the case of 1:1 $Ti(OPr)_4$:urea sample calcined at 900 °C whereas the standard sample takes more than 120 min to complete the degradation process. This enhanced efficiency is reflected in a kinetic analysis of the results. The degradation process, involving hydroxyl radical formation and subsequent degradation of the dye by the hydroxyl radical, obeys pseudo-first-order kinetics. First-order degradation rate constants, obtained by plotting the natural logarithm of the absorbance against irradiation time, are $0.27 \pm 0.02$ $min^{-1}$ for the standard sample and $0.73 \pm 0.06$ $min^{-1}$ for the urea-modified sample. A similar trend is observed with the urea-modified sample calcined at 800 °C, which has more than three times the degradation rate of the standard (Supporting Information Figure 11). An initial lag is also observed with this sample. This lag time was about 10 min for both samples and may be due to a slower adsorption of the dye onto the urea-modified sample. Dark studies, where the above experiments were repeated in the absence of a light source, were studied to eliminate any adsorption effects on the studies. Sample left for up to 24 h showed little change in absorbance. The kinetic plots and the progress of the reactions are shown in Figure 8.

The calcination temperature of the sample affects the catalytic efficiency. Both standard and urea-modified samples were

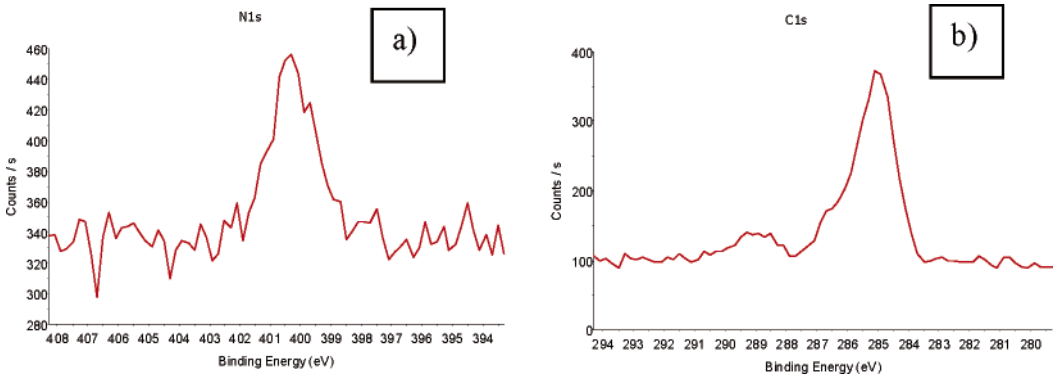


**Figure 7.** XPS plots of 1:1 $Ti(OPr)_4$:urea sample calcined at 800 °C: (a) $N_{1s}$ and (b) $C_{1s}$.

**TABLE 2: XPS Analysis of the 1:1 $Ti(OPr)_4$:Urea Sample Calcined in the Range 500−800 °C**

| $O_2$ sample Ti | $C_{1s}$/at % | O1s/at % | Ti2p/At % | N1s/at % |
|---|---|---|---|---|
| S1 500 °C | 12.2 | 63.0 | 24.4 | 0.4 |
| S2 600 °C | 12.5 | 63.2 | 23.9 | 0.5 |
| S3 700 °C | 11.3 | 63.8 | 24.4 | 0.5 |
| S4 800 °C | 11.1 | 64.0 | 24.3 | 0.5 |

calcined at 500, 600, 700, 800, and 900 °C. For the standard samples, the most efficient photocatalyst was found to be the sample calcined at 600 °C, whereas for the urea-modified sample the most efficient temperature was found to be 900 °C (Supporting Information Figure 12 and Table 1).

## 4. Discussion

Titanium tetraisopropoxide hydrolyzes vigorously with water and polycondensates of $[Ti(OH)_nX_m]^{z-}$ ions are initially formed. (When the alkoxide reacts with water the metal ion increases its coordianation by employing its vacant d-orbitals to accept oxygen lone pairs from ligands such as OH groups.) The linkage between $TiO_6^{2-}$ octahedron is formed by the dehydration reaction of $[Ti(OH)_nX_m]^{z-}$. It was previously reported that the anatase phase has an edge-shared $TiO_6^{2-}$ octahedra structure while rutile has a corner-shared octahedra.[4] The condensation reaction can also be catalyzed in acidic or basic conditions to make $TiO_6^{2-}$ octahedral from $[Ti(OH)_nX_m]^{z-}$. Urea is used here to modify the condensation reaction since gel modifiers are known to control the pore characteristics.[27] The current investigation also showed that a modifier, urea, can extend the anatase formation to higher temperatures without using any metal or metal oxide dopants. It was previously proved that the precursor processing conditions could influence significantly the high-temperature properties of various nanocrystalline metal oxides such as ZnO.[44−46] It should also be noted that the high-temperature anatase phase stability has been achieved previously by using copper sulfate as a dopant precursor.[47] However, when a precursor without any metal ions (1:1 $Ti(OPr)_4$:$H_2SO_4$) was used a major rutile phase was (63%) formed at 800 °C (Supporting Information Figure 12).

One of the major problems in the preparation of nanocrystalline $TiO_2$ is the fast reactivity of inorganic precursor toward hydrolysis and condensation.[48−50] Urea molecules chelated to the Ti ions have amino groups with a high electronegativity which retard the condensation reactions of titanium isopropoxide by altering the reaction pathway.[29] The chelation is evidenced from FTIR data which show a strong peak at 1035 $cm^{-1}$ corresponding to the Ti−O−C bond formed by the interaction between the Ti−O inorganic network and the C═O of urea (Figure 1). As the urea content is increased the chelation becomes stronger and this facilitates a stronger titania gel network. This is clearly seen from the FTIR results where the band at 1035 $cm^{-1}$ is weaker at lower urea concentration and increases in intensity with an increase in urea concentration. It has been previously reported that a gel network with little branching and cross linking with a smaller void region is morphologically weak and collapses easily on calcinations.[39] Therefore strengthening the gel network with urea assists the retention of the anatase phase to higher temperatures. Furthermore, the uniform distribution of titania precursor molecules in a urea-stabilized gel network is considered to have caused the reduction in the anatase/anatase contact points that possibly reduces the growth process of anatase particles, and this subsequently promotes pore growth.[18] Therefore the onset of the nucleation process associated with rutile formation is delayed.

The efficiency of electron−hole formation in a photocatalytic reaction is dependent on the band gap and the frequency of incident light, and how competitive electron−hole recombination is with the parallel electron−oxygen and hole−water reactions.[51−53] The anatase phase is found to be a better photocatalyst than rutile inspite of the fact that the band gap of rutile (3.0 eV) is smaller than that of anatase (3.2 eV). A faster electron−hole recombination is feasible in rutile as the recombination probability is inversely proportional to the magnitude of the band gap.[52] It has also been reported that a mixture of anatase and rutile is more photoactive than 100% anatase.[51,52] The commercial photocatalyst Degussa P-25 consisting of an anatase/rutile proportion of 70/30 is more active than pure anatase or pure rutile.[51] Various preparation methods of the sample which

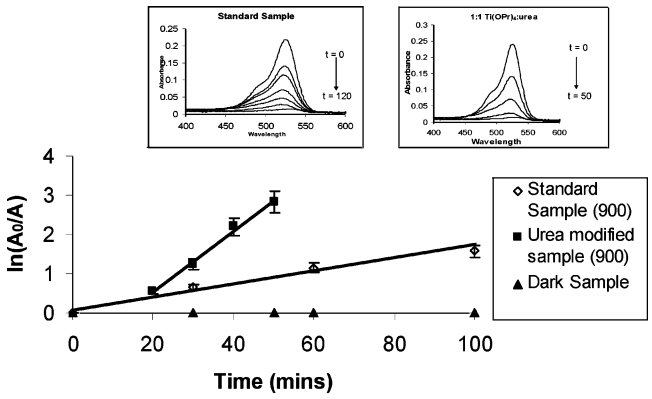


**Figure 8.** Kinetic study of standard sample and 1:1 $Ti(OPr)_4$:urea calcined sample at 900 °C. $A_0$ is the initial absorbance and $A$ is the absorbance after a time of the rhodamine dye degradation. (Error bars ±10%.) The best fit for the urea-modified sample is shown excluding the lag time. Inset: Absorption spectra of rhodamine dye degradation, using standard sample (left inset) and sample with 1:1 $Ti(OPr)_4$:urea (right inset).

result in different crystal structures or surface morphologies were also found to produce different recombination lifetimes and interfacial electron-transfer rate constants.[53−55] It has been observed in the current study that a anatase/rutile proportion of 11/89 required less than half of the time to degrade rhodamine dye compared to the 100% rutile sample. The larger amount of the anatase phase is the most likely cause for higher activity of the urea-modified sample toward the degradation of the rhodamine dye.

## 5. Conclusions

A method for making the high-temperature stable anatase phase without using any complex dopants has been reported. Ninety-seven percent anatase phase has been obtained at 800 °C with use of a 1:1 $Ti(OPr)_4$:urea composition and 11% of anatase is retained even after calcining at 900 °C. The current technique is, therefore, found to be effective in extending the anatase-to-rutile phase transformation by at least 200 °C compared to the standard samples. A significantly higher photoactivity has been achieved for sample modified using urea, calcined at 900 °C compared to the sample prepared without using urea calcined under similar conditions. Kinetic analysis shows that for the urea-modified sample at 900 °C, the decompostion rate of rhodamine 6G is almost three times faster due to the presence of the anatase phase at this temperature. This methodology is therefore suitable for the high-temperature photocatalytic application in building materials (e.g., ceramics, glass, and bricks).[21] A high-temperature stable anatase phase, good photocatalytic activity, and simplicity of processing are the main advantages of this method. The characterization of the materials has been supported by XRD, XPS, DSC, Raman, FTIR, and surface area analysis. The investigation confirmed the use of urea as a potential candidate, both as a pore-forming agent to create mesoporosity in titania and also to obtain the high-temperature stabilized anatase phase. This approach is very effective and significant to a considerable extent in dispensing with the conventional use of metal oxide dopants to retain the anatase phase at high temperatures. The transformation temperature is expected to increase at a much higher temperature with the simultaneous use of precursor modification and metal oxide dopant addition. More studies are underway in this direction.

**Acknowledgment.** This work has been carried out as part of the innovation partnership between NTera Ltd. and Dublin Institute of Technology. The authors gratefully acknowledge the financial support of Enterprise Ireland and NTera Ltd., Dublin, Ireland. P.P. and R.G. thank R&D Strand I award 2005. The authors thank Dr. Anthony Betts for his valuable comments.

**Supporting Information Available:** Tables five BET surface area analysis and XPS analysis of $Ti(OPr)_4$:urea and figures giving FTIR spectra, Raman spectra, XPS plots and XRD. This material is available free of charge via the Internet at http://pubs.acs.org.

## References and Notes

(1) Gratzel, M. *Nature* **2001**, *414*, 338.
(2) Hagfeldt, A.; Gratzel, M. *Chem. Rev.* **1995**, *95*, 49.
(3) Mills, A.; Lee, S. K. *J. Photochem. Photobiol., A* **2002**, *152*, 233.
(4) Gopal, M.; Chan, W. J. M.; Jonghe, L. C. D. *J. Mater. Sci.* **1997**, *32*, 6001.
(5) *Enclyopedia of Chemical Technology*; Mark, H. F., Othmer, D. F., Overberger, C. G., Seaberg, G. T., Eds.; John Wiley: New York, 1983; Vol. 23, p 139.
(6) Weast, R. C. *Handbook of Chemistry and Physics*; CRC Press: Boca Raton, FL, 1984; p B-154.
(7) Kostov, I. *Minerology*, 3rd ed.; Nauka, Izkustia, Sofia, 1973.
(8) Yang, S. W.; Gao, L. *J. Am. Ceram. Soc.* **2005**, *88*, 968.
(9) (a) Karakitsou, K. E.; Verykios, X. E. *J. Phys. Chem.* **1993**, *97*, 1184. (b) McLoughlin, O. A.; Kehoe, S. C.; McGuigan, K. G.; Duffy, E. F.; Touati, F. A.; Gernjak, W.; Alberola, I. O.; Rodríguez, S. M.; Gill, L. W. *Solar Energy* **2004**, *77*, 657.
(10) (a) Addamo, M; Augugliaro, V.; Paola, D. A.; Lopez, G. E.; Loddo, V.; Marci, G.; Molinari, R.; Palmisano, L.; Schiavello, M. *J. Phys. Chem. B* **2004**, *108*, 3303. (b) Lonnen, J.; Kilvington, S.; Kehoe, S. C.; Touati, F. A.; McGuigan, K. G. *Water Res.* **2005**, *39*, 877.
(11) Hu, C.; Lan, Y.; Hu, X.; Wang, A. *J. Phys. Chem. B* **2006**, *110*, 4066.
(12) Sakatani, Y.; Grosso, D.; Nicole, L.; Boissiere, C.; Illia, S.; Sanchez, C. *J. Mater. Chem.* **2006**, *16*, 77.
(13) Fujishima, A.; Rao, T. N.; Tryk, D. A. *J. Photochem. Photobiol., C* **2001**, *1*, 1.
(14) Parkin, I. P.; Palgrave, R. G. *J. Mater. Chem.* **2005**, *15*, 1689.
(15) Mills, A.; Lee, S. K. *J. Photochem. Photobiol., A* **2006**, *182*, 181.
(16) Zzanderna, A. W.; Rao, C. N. R.; Honig, J. M. *Trans. Faraday Soc.* **1958**, *54*, 1069.
(17) Yoganarasimhan, S. R.; Rao, C. N. R. *Trans. Faraday Soc.* **1962**, *58*, 1579.
(18) Kumar, S. R.; Pillai, S. C.; Hareesh, U. S.; Mukundan, P.; Warrier, K. G. K. *Mater. Lett.* **2000**, *43*¸ 286.
(19) Reidy, D. J.; Holmes, J. D.; Morris, M. A. *J. Eur. Ceram. Soc.* **2006**, *26*, 1527.
(20) Navrotsky, A.; Kleppla, O. J. *J. Am. Ceram. Soc.* **1967**, *50*, 626.
(21) Machida, M.; Norimoto, W. K.; Kimura, T. *J. Am. Ceram. Soc.* **2005**, *88*, 95.
(22) Rao, C. N. R.; Turner, A.; Hanig, J. M. *J. Phys. Chem.* **1959**, *11*, 173.
(23) Ranjit, K. T.; Willner, I.; Bossmann, S. H.; Braun, A. M. *Environ. Sci. Technol.* **2001**, *35*, 154.
(24) Reidy, D. J.; Holmes, J. D.; Nagle, C.; Morris, M. A. *J. Mater. Chem.* **2005**, *15*, 3494.
(25) Kumar, K. N. P.; Kiezer, K.; Burggraaf, A. *J. Mater. Chem.* **1993**, *3*, 141.
(26) Baiju, K. V.; Sibu, C. P.; Rajesh, K.; Pillai, P. K.; Mukundan, P.; Warrier, K. G. K.; Wunderlich, W. *Mater. Chem. Phys.* **2005**, *90*, 123.
(27) Suresh, C.; Biju, V.; Mukundan, P.; Warrier, K. G. K. *Polyhedron* **1998**, *17*, 3131.
(28) Khimich, N. N.; Venzel, B. I.; Drozdova, I. A.; Koptelova, L. A. *Russ. J. Appl. Chem.* **2002**, *75*, 1108.
(29) Cheng, P.; Qiu, J.; Gu, M.; Shangguan, W. *Mater. Lett.* **2004**, *58*, 3751.
(30) Yuan, J.; Chen, M.; Shi, J.; Shangguan, W. *Int. J. Hydrogen Energy* **2006**, *31*, 1326.
(31) Yin, S.; Ihara, K.; Aita, Y.; Kommatsu, M.; Sato, T. *J. Photochem. Photobiol., A* **2006,** *179*, 105.
(32) Zheng, J. Y.; Pang, J. B.; Qiu, K. Y.; Wei, Y. *Microporous Mesoporous Mater.* **2001**, *49*, 189.
(33) Bakardjieva, S.; Subrt, J.; Stengl, V.; Dianez, M. J.; Dianez, M. J. S.; Sayagues, M. J. *Appl. Catal., B* **2005**, *58*, 193.
(34) Yin, S.; Aita, Y.; Komatsu, M.; Sato, T. *J. Eur. Ceram. Soc.* **2006**, *26*, 2735.
(35) Sakthivel, S.; Janczarek, M.; Kisch, H. *J. Phys. Chem. B* **2004**, *108*, 19384.
(36) Yates, H. M.; Nolan, M. G.; Sheel, D. W.; Pemble, M. E. *J. Photochem. Photobiol., A* **2006**, *179*, 213.
(37) Yamamoto, Y.; Moribe, S.; Ikoma, T.; Akiyama, K.; Zhang, Q.; Saito, F.; Kubota, S. T. *Mol. Phys.* **2006**, *104*, 1733.
(38) Spurr, R. A.; Myers, H. *Anal. Chem.* **1957**, *29*, 760.
(39) Kung, H. H.; Ko, E. I. *Chem. Eng. J.* **1996**, *64*, 203.
(40) Ren, L.; Huang, X.; Sun, F.; He, X. *Mater. Lett.* DOI: 10.1016/j.matlet.2006.04.097.
(41) Shi, Z. M.; Ye, X. Y.; Liang, K. M.; Gu, S. R.; Pan, F. *J. Mater. Sci.* **2003**, *22*, 1255.
(42) Irie, H.; Watanabe, Y.; Hashimoto, K. *J. Phys. Chem. B* **2003**, *107*, 5483.
(43) Cheng, X.; Lou, Y.; Samia, A. C. S.; Burda, C.; Gole, J. L. *Adv. Funt. Mater.* **2005**, *15*, 41.
(44) Pillai, S. C.; Kelly, J. M.; McCormack, D. E.; Ramesh, R. *J. Mater. Chem.* **2004**, *14*, 1572.
(45) Pillai, S. C.; Kelly, J. M.; McCormack, D. E; O'Brien, P.; Ramesh, R. *J. Mater. Chem.* **2003**, *13*, 2586.
(46) Pillai, S. C.; Kelly, J. M.; McCormack, D. E.; Ramesh, R. *Mater. Sci. Technol.* **2004**, *20*, 964.
(47) Bokhimi, X.; Morales, A.; Novaro, O.; López, T.; Chimal, O.; Asomoza, M.; Gómez, R. *Chem. Mater.* **1997**, *9*, 2616.

(48) Pillai, S. C.; Boland, S. W.; Haile, S. M. *J. Am. Ceram. Soc*. **2004**, *87*, 1388.

(49) Boland, S. W.; Pillai, S. C.; Yang, W. D.; Haile, S. M. *J. Mater. Res.* **2004**, *19*, 1492.

(50) Sibu, C. P.; Kumar, S. R.; Mukundan, P.; Warrier, K. G. K. *Chem. Mater*. **2002**, *14*, 2876.

(51) (a) Abe, R.; Sayama, K.; Domen, K.; Arakawa, H. *Chem. Phys. Lett.* **2001**, *344*, 339. (b) Carp, O.; Huisman, C. L.; Reller, A. *Prog. Solid State Chem.* **2004**, *32*, 33.

(52) Gandhe, A. R.; Naik, S. P.; Fernades, J. B. *Microporous Mesoporous Mater*. **2005**, *87*, 103.

(53) Hoffmann, M. R.; Martin, S. T.; Choi, W.; Bahanemann, D. W. *Chem. Rev.* **1995**, *95*, 69.

(54) Acosta, D. R.; Martinez, A. I.; Lopez, A. A.; Magana, C. R. *J. Mol. Catal. A*: *Chem.* **2005**, *228*, 183.

(55) Baiju, K. V.; Periyat, P.; Pillai, P. K.; Mukundan, P.; Warrier, K. G. K.; Wunderlich, W. *Mater. Lett*. DOI: 10.1016/j.matlet.2006.07.124.